Noise considerations in Water-Fat Separation with Bipolar Multi-echo Sequences

W. Lu[1], H. Yu[2], A. Shimakawa[2], M. Alley[1], S. Reeder[3], and B. Hargreaves[1]

[1]Radiology, Stanford University, Stanford, CA, United States, [2]2Global Applied Science Laboratory, GE Healthcare, Menlo Park, CA, United States, [3]Biomedical Engineering, University of Wisconsin-Madison, Madison, WI, United States

Introduction: Bipolar multi-echo sequences (Fig. 1(a)) provide an efficient means to acquire multiple echoes in a single repetition for water-fat separation, which leads to shorter scan times, higher SNR-efficiency, and reduced motion-induced artifacts. One major technical problem is that the chemical-shift-induced misregistration between water and fat exists in opposite readout directions between even and odd echoes. It has been demonstrated in [1] that separating water/fat signals in *k*-space effectively eliminates the chemical-shift induced misregistration. Specifically, after correcting *k*-space echo misalignment and field-inhomogeneity-induced misregistration [1], the image-domain data can be Fourier transformed into the following k-space signal model:

$$\underbrace{\begin{pmatrix} S_1(k_x,k_y) \\ S_2(k_x,k_y) \\ S_3(k_x,k_y) \end{pmatrix}}_{\mathbf{S}} = \underbrace{\begin{pmatrix} 1 & e^{i2\pi\Delta f t_1(k_x,k_y)} \\ 1 & e^{i2\pi\Delta f t_2(k_x,k_y)} \\ 1 & e^{i2\pi\Delta f t_3(k_x,k_y)} \end{pmatrix}}_{A} \underbrace{\begin{pmatrix} S_W(k_x,k_y) \\ S_F(k_x,k_y) \end{pmatrix}}_{\Gamma}$$

S_W: *k*-space water sample
S_F: *k*-space fat sample

The *k*-space separation is done via $\hat{\Gamma} = A^{\dagger}\mathbf{S}$ where $A^{\dagger} = (A^{\mathbf{H}}A)^{-1}A^{\mathbf{H}}$. For each *k*-space location, the matrix *A* depends on the corresponding acquisition times. As shown in Fig. 1(b), the acquisition times at (k_x, k_y) are placed in an asymmetric pattern. That is, t_3-$t_2 \neq t_2$-t_1 except at k_x=0. Therefore, the *k*-space separation results in different noise amplification for different *k*-space locations. In this work, we characterize the colored noise present in separated water/fat images with a noise amplification factor, and demonstrate the utility of the noise amplification factor in choosing imaging parameters or regularization parameters in the case of ill-conditioned separation.

Theory: The *k*-space signal model can be extended by including a noise vector **n**: $\mathbf{S}+\mathbf{n}=A\mathbf{\Gamma}$ where **n** models acquisition noise as zero-mean white Gaussian noise: i.e., $\mathbf{n}\sim N(\mathbf{0}, \sigma^2\mathbf{I})$, where σ^2 is the variance of each element in **n** and **I** is an identity matrix. The effect of the noise vector **n** on the least-squares solution can be accounted for by the following noise amplification factor:

$$\eta = \frac{trace(A^{\dagger}\Sigma(A^{\dagger})^{\mathbf{H}})/2}{\sigma^2/3}$$

where the numerator is the variance of the noise present in the least-squares solution, and the denominator is the lowest achievable noise variance with a three-point acquisition. Hence, $\eta \geq 1$.

Method: To verify the utility of the noise amplification factor in selecting imaging parameters, we first used a bipolar multi-echo sequence to scan the knee of a healthy volunteer at 1.5 T with an 8-channel coil and the imaging parameters: matrix 240x240, FOV 16 cm, TR=14.86 ms, $TE_{1,2,3}$=2.6, 5.9, 9.2 ms and BW 41.67 kHz (Case I in Fig. 2.) Another knee study was performed at 1.5 T with an extremity coil and the imaging parameters: matrix 256x256, FOV 20 cm, TR=11 ms, $TE_{1,2,3}$=3.1, 5.3, 7.5 ms and BW 62.5 kHz (Case II in Fig. 2.) The imaging parameters in Case I result in small variation of noise amplification, while in Case II high-frequency noise is greatly amplified due to both insufficient water-fat phase differences developed at the boundary of the zigzag trajectory and the fact that the first and third echoes are nearly identical.
The small difference among three acquisitions leads to an ill-conditioned inverse problem for separating *k*-space samples in high-frequency regions. To address the ill-conditioned separation, Tikhonov regularization is incorporated with the *k*-space separation in the high-frequency regions. Specifically, for the *k*-space locations where the noise amplification factor is large, the pseudo-inverse $A^{\dagger}$ is replaced with $A^{\dagger\dagger} = (A^{\mathbf{H}}A+\kappa\mathbf{I})^{-1}A^{\mathbf{H}}$. In our implementation, the regularization parameter, κ, is set such that the factor $\eta \leq 2$. In general, no regularization is needed for the regions near the k-space center, where the k-space separation is well-conditioned. Fig. 2 (c) shows the plot of the noise amplification factor after the regularization incorporated in Case III. In this case, without changing the imaging parameters used in Case II, the regularization significantly reduced the factor in the high-frequency regions.

Results: The sequence was implemented on a GE 1.5 T scanner. Fig. 3 (a,b) shows the comparison between the separated water images obtained from an image-domain method [2] and the *k*-space separation method. It can be seen that the image parameters used in Case I enable the *k*-space separation to eliminate the chemical-shift-induced artifacts without incurring noticeable noise amplification. In contrast, Fig. 4(b) shows that the imaging parameters used in Case II causes the *k*-space separation to generate significant high-frequency noise in the separated image. Incorporating the regularization with the *k*-space separation eliminates not only the chemical–shift-induced artifacts but also the high-frequency noise (see Fig. 4(c)).

Conclusion: A noise amplification factor is proposed to characterize the noise performance of the *k*-space separation with bipolar multi-echo sequences. Its utility in choosing imaging parameters and regularization parameters has been demonstrated with *in vivo* results.

References: 1. W. Lu, et al. ISMRM, 2007. 2. Reeder S., et al. MRM2004 51(1):123-30. 3. P. Koken, et al. ISMRM, 2007. 4. Wieben O., et al. ISMRM, 2005.

Funded by NIH RR009784. EB002524.

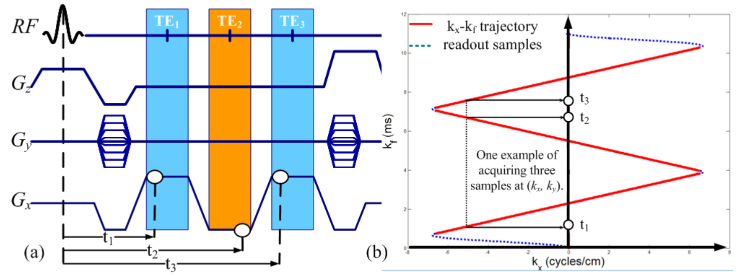

Fig.1: (a) Diagram of a bipolar multi-echo sequence, and (b) its corresponding *k*-space trajectory in k_f-k_x space. Note the asymmetric sampling pattern; i.e., t_3-$t_2 \neq t_2$-t_1 except at k_x=0.

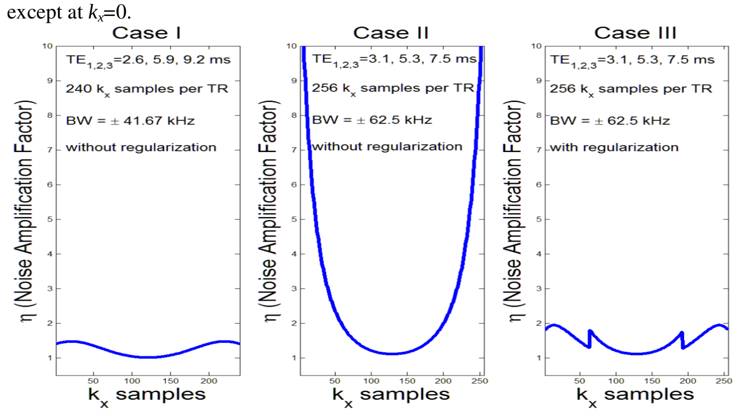

Fig.2: Comparison of the noise amplification variation resultant from the imaging parameters used in Case I and Case II. With the same parameters used in Case II, the regularization used in Case III reduces the factor in high-frequency regions.

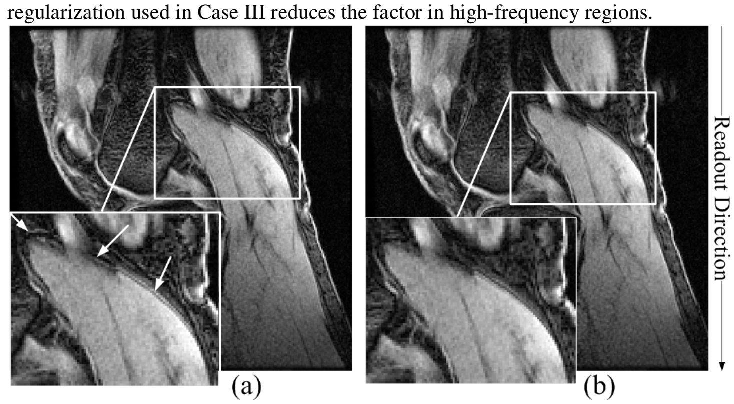

Fig. 3: Comparison of separated water images of a knee study (Case I) using (a) an image-domain method, and (b) the k-space method. The artifacts identified with arrows in (a) are suppressed in (b) without incurring noticeable noise amplification.

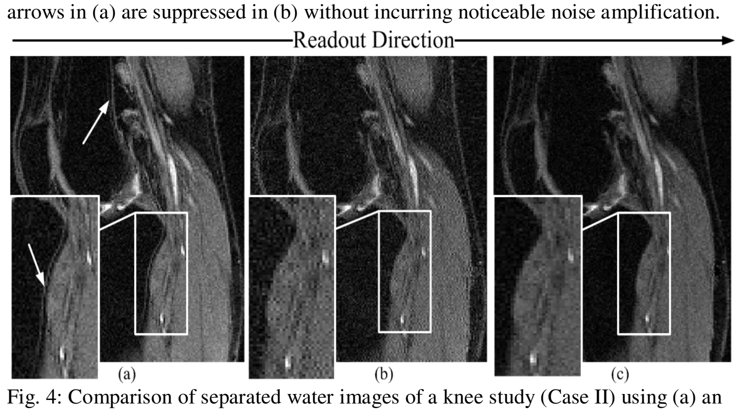

Fig. 4: Comparison of separated water images of a knee study (Case II) using (a) an image-domain method, and the *k*-space methods (b) without and (c) with Tikhonov regularization. The artifacts identified with arrows in (a) are eliminated in (b). The high-frequency noise in (b) is suppressed in (c), as anticipated by the variation of noise amplification factor in Case III of Fig. 2.